

CHANGES IN MOLECULAR BIOMARKER AND BULK CARBON SKELETAL PARAMETERS OF VITRINITE CONCENTRATES AS A FUNCTION OF RANK.

Gordon D. Love*, Colin E. Snape* and Andrew D. Carr[‡]

* University of Strathclyde, Department of Pure & Applied Chemistry,
Glasgow G1 1XL, UK.

[‡] British Gas plc, London Research Station, Michael Road, London SW6 2AD, UK.

Keywords: Biomarkers, Vitrinite Reflectance, Solid State ¹³C NMR.

ABSTRACT

A sequential extraction scheme to differentiate between molecular alkanes and those covalently-bound to the macromolecular structure has been applied to a suite of vitrinite concentrates handpicked from six UK bituminous coals covering the rank range (%R_o = 0.46-1.32 at 546 nm). The aim was to ascertain whether the biomarker indices (i) were consistent with the measured vitrinite reflectance values, especially for the lower rank members of the suite where reflectance measurements are unreliable and (ii) differ markedly for the easily extractable, clathrated and covalently-bound phases. The quantitatively reliable single pulse excitation (SPE) solid state ¹³C NMR technique has also been used to elucidate the changes in the bulk vitrinite structure across the relatively narrow rank range investigated. Although both hopane and methylphenanthrene parameters for easily extractable species are sensitive to small variations in vitrinite reflectance, significant variations have been found between the biomarker parameters for easily extractable, clathrated and covalently-bound material. In general, restricted motions in the macromolecular structure make the latter less mature, as reflected by hopane and phenanthrene parameters, than the easily extractable and clathrated molecular species. Solid state ¹³C NMR revealed that the variations in carbon aromaticity and the degree of condensation of the aromatic structure occurring in the %R_o range of ca 0.45-0.80 are relatively small.

INTRODUCTION

Biological markers are compounds detected in the geosphere derived from living organisms whose basic carbon skeleton has survived the processes of diagenesis and thermal maturation. The most commonly studied biomarkers are the cyclic alkanes; the hopanes and the steranes, which are derived from hopanoid and steroid natural products respectively, and are ubiquitous components of crude oils, kerogens and coals. As well as providing information about the original biological input to sediments, the distribution of certain hopane and sterane stereoisomers have been widely used to indicate the thermal stress experienced by fossil organic matter (see, for example, Fu Jiamo et al (1), Chaffee et al (2) and Mackenzie (3) and references therein for comprehensive reviews). The biologically synthesised conformations of their precursors are not the most thermally stable and configurational isomerisation is observed at certain chiral centres as maturation proceeds. Although these biomarkers are generally only present in small quantities (<< 1% w/w) in solvent extracts and pyrolysates, they are readily detectable using single ion monitoring in gas chromatography-mass spectrometry (GC-MS) without the need for extensive pre-separation (1-3).

To summarise, the hopanes are pentacyclic triterpanes which are believed to be derived from a C₃₅ triterpene alcohol, bacteriohopane-tetrol, a constituent of the membranes of bacteria other than Archaeobacteria. A series of C₂₇-C₃₅ hopanes is the most commonly observed distribution in ancient sediments but usually the C₂₈ member is missing (1-3). The biological 17β(H), 21β(H) configuration inherited by the alkanes of immature sediments is lost rapidly with increasing maturity forming a mixture of 17α(H), 21β(H) and 17β(H), 21α(H) stereochemistries. Eventually the 17β(H), 21α(H)-hopanes also convert to the 17α(H), 21β(H) form. The sterol precursors of the tetracyclic steranes are widely distributed in nature and the most commonly encountered

steranes are those of carbon number C₂₇, C₂₈ and C₂₉ although variable amounts of C₂₁ and C₂₂ isomers with shorter alkyl sidechains are also often present. At the later stages of diagenesis, the main steroidal components are usually alkanes and Ring C monoaromatics. Further maturation leads to configurational isomerisation, aromatisation of C-ring monoaromatic steroids to ABC-ring triaromatics (substituted phenanthrenes, see below) and enrichment of the lower molecular weight (MW) components (C₂₀-C₂₂) relative to the higher MW counterparts (C₂₆-C₂₉).

The Methylphenanthrene Index (MPI) proposed by Radke et al.⁽⁴⁾ is a widely used maturity parameter based on their distribution in solvent extracts. Steroids and triterpenoids are probable biological precursors with their degradation and aromatisation yielding only 1- and 2- MP isomers. The 3- and 9-MPs arise as a result of methylation of phenanthrene and rearrangement of mono-methyl phenanthrenes. Radke et al.⁽⁴⁻⁶⁾ observed that the relative amounts of 2- and 3- MP increase compared to the 1- and 9- isomers with increasing burial and depth. An empirical correlation (MPI 1, see Table 3) was then devised based on the distribution of these compounds relative to the amount of phenanthrene which could predict vitrinite reflectance values (% R_c) for the samples studied.

The above molecular indices are usually calculated by observing the distribution of the appropriate biomarkers obtained by low temperature extraction using chloroform, dichloromethane (DCM) or methanol (or their mixtures). Since this type of treatment removes only a small proportion of the total organic matter (usually <5% w/w), it does not follow that the distributions of biomarkers are necessarily representative of those covalently bound to the macromolecular structure. Indeed, previous studies using low severity catalytic hydrogenation have established that in lignites⁽⁷⁾, kerogens⁽⁸⁾ and a high volatile bituminous coal⁽⁷⁾, hopanes and steranes can be incorporated into the polymeric backbone via functional groups present in the original biolipids whilst retaining their less thermodynamically stable biological configurations. Thus, it appears that compounds covalently bound to the macromolecular network may be less sensitive to thermal alteration. Furthermore, it is known that coals contain a significant amount of physically trapped, low MW moieties which are inaccessible to treatment with the solvents mentioned above⁽⁹⁻¹¹⁾. However, these components can partly be removed when more powerful solvents like pyridine or binary solvent mixtures⁽¹²⁾ destroy the stronger non-covalent interactions within the macromolecular matrix⁽¹³⁾. This phase may contain significant amounts of biomarker species which may have a different distribution to those detected in the usual solvent or hydrogenation extracts. This prompted the authors to develop a sequential degradation scheme to help differentiate between easily extractable and clathrated species and moieties which were covalently-bound through weak heteroatomic bonds or more stronger C-C bonds. After an initial DCM soxhlet extraction, refluxing in pyridine allows the removal of more occluded material. Mild batchwise hydrogenation using a dispersed sulphided molybdenum (Mo) catalyst is then performed to cleave weak ester, ether and sulphide linkages. A final hydrolysis step in a fixed-bed reactor using a hydrogen sweep gas can render a significant proportion of the organic residue soluble in DCM (typically over 50% daf basis).

The sequential scheme has been applied here to a suite of vitrinite concentrates handpicked from six UK bituminous coals covering the rank range (%R_o = 0.46-1.32 at 546 nm) which corresponds to a maturity range from just before to just after the so called "oil-generating window" for Type III materials. The aim of this investigation has been to ascertain whether the biomarker indices (i) were consistent with the measured %R_o values, especially for the lower rank members of the suite where reflectance measurements are unreliable and (ii) differ markedly for the easily extractable, clathrated and covalently-bound phases.

As indicated above, the chemically-bound moieties appear to be more resistant to geothermal stress than molecules in the bitumen phase suggesting that a detailed chemical analysis of solvent extracts may not give a valid representation of the total organic structure. Thus, solid state ¹³C NMR has been used to elucidate the changes in the bulk vitrinite structure across the relatively narrow rank range using the quantitatively reliable single pulse excitation (SPE) measurements. Previous investigators have correlated vitrinite reflectance with aromaticities derived from cross polarisation

(CP) (14-17), but it is now generally accepted that CP can strongly discriminate against aromatic carbons in fossil fuels (17-19).

EXPERIMENTAL

The proximate and ultimate analyses, maceral compositions and measured average vitrinite reflectance values for the samples investigated are summarised in Table 1.

Solvent Extractions Each sample was ground to <150 μ m, dried in a vacuum oven at 50°C for 24 hours and then Soxhlet extracted with dichloromethane (DCM) for 72 hours. The solid residue (2-5g) was then refluxed rapidly with 200 cm³ boiling pyridine (3 x 45 mins). The soaking time in pyridine was relatively short to prevent the structure rearranging to a more tightly bound conformation due to the formation of more non-covalent interactions (21). After each reflux step, the solids were washed in a DCM/ methanol solvent mixture (3:1 v/v) and then dried *in vacuo* to remove as much entrained pyridine as possible.

Catalytic Hydrogenation and Fixed-Bed Hydrolysis Catalyst impregnation of solvent-extracted vitrinites was performed as described previously (22) with aqueous / methanol solutions of the precursor, ammonium dioxodithiomolybdate [(NH₄)₂MoO₂S₂], to give a nominal Mo loading of 1% daf coal. Batchwise hydrogenation runs were conducted at 300°C and 70 bar hydrogen pressure (ambient) in 7 cm³ stainless steel microreactors constructed from Autoclave Engineers fittings. The microreactors were immersed in a fluidised sandbath for 60 mins. After cooling the reaction products were recovered in DCM, refluxed and then filtered to remove the DCM-insoluble residues and to determine overall conversions. The procedure for temperature-programmed hydrolysis has been described in detail elsewhere (22)

Product Work-up and Analysis The DCM-soluble products from each stage of the extraction procedure were dried to constant weight in a stream of dry nitrogen. These were then separated by open-column silica gel adsorption chromatography into alkanes, aromatics and polars by eluting successively with n-hexane, n-hexane-toluene (1:1 v/v) and DCM/methanol (2:1 v/v). The yields were determined by transferring relatively concentrated solutions of the fractions into pre-weighed screw-cap vials and evaporating the residual solvent under a stream of nitrogen. GC-MS analysis was performed on the alkane and aromatic fractions using a Finnigan MAT TSQ70 coupled to a Varian 3400 GC. For the alkanes, the single ions monitored were m/z 191 (for triterpanes) and 217 (for steranes). The sterane standards, 5 β (H)-cholane and 20-methyl-5 α (H)-pregnane (Chiron Labs, Trondheim), was added to selected samples before injection.

Solid State ¹³C NMR Spectroscopy All the ¹³C NMR measurements were carried out at 25 MHz on a Bruker MSL100 spectrometer with MAS at 4.5-5.0 kHz to give spectra in which the sideband intensities are only ca 3% of the central aromatic bands. The vitrinites were vacuum dried and then ca 250 mg of sample was packed into the zirconia rotors. The ¹H decoupling and spin-lock field was ca 60 kHz and, for SPE, the 90° ¹³C pulse width was 4.5 μ s. ¹³C thermal relaxation times (T_{1s}) of the vitrinites were determined using an appropriate CP pulse sequence with a contact time of 5 ms in most cases.

A relaxation delay of 20 s was used for the variable delay SPE DD measurements for Snibson where the ¹³C T_{1s} were relatively short. In this case, up to ten dephasing periods in the range of 1 to 200 μ s were used before the first rotational modulation. However, for the other samples with ¹³C T_{1s} much longer than 5 s, a recycle time of either 100 or 120 s was used in the SPE DD experiment with, due to the sensitivity limitations, only a single delay of 60 μ s. In order to check that the tuning had remained virtually constant throughout the duration of all the DD experiments, the delays were arranged in a random order and between 1000 and 3000 scans were accumulated for each delay. No background signal was evident in the SPE spectra from the Kel-F rotor caps. All the FIDs were processed using a line broadening factor of either 50 or 100 Hz. The

Table 1 Analyses of the vitrinite concentrates

	Vitrinites					
	Snibson	Blidworth	Silkstone	Manton	Nantgarw	Oakdale
% moisture (ad)	8.9	4.1	13.4	4.0	1.1	1.5
% ash (dry basis)	2.7	1.6	1.3	1.1	2.4	7.8
% dmmf C	79.0	80.4	82.6	81.8	88.9	85.8
" " H	5.0	5.0	5.1	5.1	4.9	4.3
" " N	1.6	1.5	1.7	1.8	1.7	1.5
% Total S, dry basis	<0.3	<0.3	1.1	0.58	0.35	0.46
H/C ratio	0.76	0.75	0.74	0.74	0.66	0.61
Vitrinite reflectance, R _o % av.	0.47	0.59	0.66	0.79	1.08	1.32
Maceral comp.						
Liptinite	7.6	8.0	7.4	9.0	0.4	2.0
% v/v Vitrinite	87.8	90.0	88.2	89.6	93.4	93.6
Inertinite	4.6	2.0	4.4	1.4	6.2	4.4

ad = as determined.

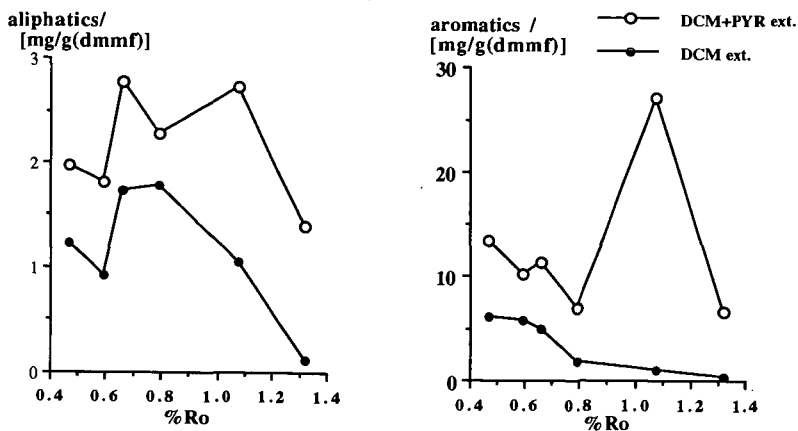


Figure 1 Yields of alkanes and aromatics from DCM and pyridine extraction stages as a function of vitrinite reflectance.

measurement of aromatic and aliphatic peak areas manually was found to be generally more precise than using the integrals generated by the spectrometer software.

RESULTS AND DISCUSSION

Fraction yields Inspection of Figure 1 showing the yields of the total aliphatic and aromatic fractions recoverable with DCM and the cumulative yields following the subsequent pyridine reflux indicates that a substantial amount of low MW material is indeed clathrated within the vitrinite macromolecular structure across the rank range. Such material is contained in the closed pores of the vitrinite according to Radke et al.⁽²⁴⁾ and, as the rank increases, these will account for greater proportions of the decreasing overall pore volume. This explains the relatively large amounts of aromatic species which are accessible to pyridine but not to DCM extraction especially at higher rank. Aromatic species are more strongly retained than the alkanes (Figure 1) which would appear to be more easily forced through the pores and into the easily extractable bitumen. Nantgarw ($\%R_o = 1.08$) represents a maturity where the principal cracking reactions have occurred but, relatively, condensation of aromatic moieties is in its infancy giving rise to the highest yield of pyridine-extractable aromatics (Figure 1).

The yields of alkanes and aromatics in the range 0.1-0.5% (dmmf basis) from catalytic hydrogenation were comparable to those from pyridine extraction but did not vary systematically across the rank range. As anticipated, the hydrogenation yields for the vitrinites were considerably lower than those obtained previously for a Type I and a Type II kerogen due to the lower concentrations of labile C-O and C-S bonds⁽²⁶⁾.

Biomarker profiles The various aliphatic and aromatic biomarker maturity parameters are listed in Table 2 which indicates that those for the DCM-extractable phase correlate to varying degrees with vitrinite reflectances. In particular, the following trends with increasing $\%R_o$ can be noted.

- (i) The MPI increases and the calculated vitrinite reflectances are in remarkably good agreement with the actual values.
- (ii) The hopane C_{22} and sterane C_{20} S/S+R ratios are sensitive to changes in vitrinite reflectance before the oil-generating window (Snibson-Silksworth, $\%R_o$ 0.47-0.66) with the sterane ratio extending somewhat further up to Manton.
- (iii) The C_{30} $\beta/\alpha\beta$ ratio decreases steadily with increasing rank.

These trends would hence appear to be representative of the geothermal stress experienced by the organic matter.

In the pyridine extracts the distribution of biomarkers with respect to their DCM counterparts would appear to be rank dependent. For the lowest rank members of the suite, Snibston and Blidworth, the aliphatic indices show a slightly more mature profile (Table 2) which could arise from the catalytic effects of the small amounts of minerals present⁽²⁵⁾ on an otherwise homogeneous distribution. Such material in intimate contact with the mineral matrix is often designated as the "bitumen 2" in oil shales and clays⁽²⁶⁾. More interestingly at higher rank (Nantgarw and Oakdale), some components in the clathrated phase seem to represent those which have been more recently cleaved from the macromolecular framework. These are conspicuous by their relatively immature conformation (Table 2) having been preserved in the macromolecule by covalent bonding till release at higher maturity. For example, the higher MW members of the extended hopane series which are usually lost rapidly with thermal maturation are observed more prominently in the pyridine extractable alkanes than in those recovered by DCM treatment, even for the Oakdale vitrinite. In terms of detecting such immature biomarker distributions in the clathrated phase, Silkstone marks the cross-over point in this suite of samples. Although significant proportions of the biomarkers identified may well be derived from the small amounts of liptinite present (Table 1), it appears that their accessibility to solvents is governed by the changes in the bulk, i.e. vitrinite structure as a function of rank.

Table 2. Selected Aliphatic and Aromatic Biomarker Maturity Parameters

SAMPLE	STAGE	Aliphatics					Aromatics			
		C ₃₁ αβ a	C ₃₂ αβ b	C ₃₀ c β/αβ	C ₂₇ β/α d	T _s / T _m e	C ₂₉ ααα f	MPI 1 g	%R _c h	MPI i
Snibston	DCM	0.46	0.32	0.63	0.78	0.00	0.11	0.15	0.49	trace
	PYR	0.48	0.38	0.44	0.49	0.08	0.22	P	N.A.	trace
	HYD	0.30	0.24	1.03	0.67	0.00	0.22	P	N.A.	trace
Blidworth	DCM	0.60	0.55	0.46	0.09	0.00	0.36	0.34	0.60	1.04
	PYR	0.56	0.56	0.44	0.09	0.07	0.39	P	N.A.	trace
	HYD	0.40	0.42	0.47	0.29	0.11	0.26	P	N.A.	trace
Silkstone	DCM	0.58	0.57	0.37	0.07	0.03	0.43	0.41	0.65	1.10
	PYR	0.51	0.55	0.39	0.07	0.00	0.44	0.31	0.59	1.17
	HYD	0.52	0.52	0.40	0.23	0.13	0.36	0.16	0.50	trace
Manton	DCM	0.60	0.59	0.32	0.09	0.03	0.48	0.63	0.78	1.10
	PYR*	0.60	0.59	0.30	0.11	0.03	0.46	0.68	0.81	0.90
	DCM	0.56	0.51	0.13	0.30	0.74	0.48	1.07	1.05	2.15
Nangarw	PYR*	N.D.	N.D.	N.D.	N.D.	N.D.	N.D.	1.06	1.04	1.96
	HYD	0.51	0.54	0.36	0.91	0.63	0.37	1.11	1.07	1.91
	DCM	0.57	0.58	0.07	0.00	0.45	0.50	1.52	1.31	3.34
Oakdale	PYR	0.57	0.62	0.07	0.00	0.38	0.44	0.94	0.96	2.71

KEY

DCM = dichloromethane extraction, PYR = pyridine reflux, CAT = catalytic hydrogenation. (see experimental for details).
 N.D. = Not determined. * = not sequentially extracted. N.A. = Not available.
 a: α,β - homohopane 22S/ 22S+22R. Starting value 0, end value 0.5-0.6 (attained before oil generating period)
 b: α,β - bishomohopane 22S/ 22S+22R. Starting value 0, end value 0.5-0.6 (attained before oil generating period)
 c: C₃₀ moretane/ α,β - hopane. In this rank range, the lower the value, the greater the maturity.
 d: C₂₇ 17β(H)- 22, 29, 30-trisnorhopane / 17α(H)- 22, 29, 30-trisnorhopane. At lower ranks, higher values indicate low maturities.
 e: C₂₇ 18α(H)- 22, 29, 30-trisnorhopane / 17α(H)- 22, 29, 30-trisnorhopane. At higher ranks, higher values indicate high maturities.
 f: C₂₉ ααα - sterane 20S/ 20S+20R. Starting value 0, end value around 0.5. Extends further into the oil window than parameters (a) & (b).
 g: MPI 1 = 1.5 ((2-MP)+[3-MP]) / ((P)+[1-MP]+[9-MP]) where [P] and [MP] denote phenanthrene and methylphenanthrene respectively.
 h: P in table indicates that the amount of phenanthrene detected far exceeded the concentrations of all methylphenanthrenes.
 i: The predicted vitrinite reflectance from MPI 1, R_c(%) = 0.60 MPI 1 + 0.40 (for MPR < 2.65)
 I: MPR = [2-MP] / [1-MP], 'trace' indicates small, unresolvable contributions from all methylphenanthrenes.

The use of the sterane internal standards has indicated semi-quantitatively that the amounts of molecular (DCM- and pyridine-extractable) hopanes and steranes decrease markedly with increasing rank. However, this depletion is substantially less marked when one takes account of the significant amounts released by the hydrogenation step (see above).

Biomarkers such as C₃₁ and C₃₂ α,β-hopanes with the 22R configuration, C₂₇ 17β (H) - 22, 29, 30-trisnorhopane and C₂₉ (α,α,α-20R) steranes can be extracted from peats during early diagenesis (7) and all are detected in higher proportions than expected in the hydrogenation products, even for the highest rank of vitrinite (Nantgarw) to which this step has been applied (Table 2). This confirms that configurations can be preserved through incorporation of biolipids into the macromolecular structure during early diagenesis and this holds for both chiral centres which are part of a ring or in an alkyl sidechain.

Carbon skeletal parameters Table 3 summarises the carbon skeletal parameters obtained from the SPE ¹³C NMR measurements. Due to the time consuming nature of these experiments, only results for 4 of the samples have been obtained thus far. As a check on the self-consistency of both the aromaticities and the non-protonated aromatic carbon concentrations obtained for the vitrinite concentrates, their aliphatic H/C ratios have been derived using the following relationship (23):

$$(H/C)_{\text{overall}} = (H/C)_{\text{ali}}(1 - f_a) + (H/C)_{\text{ar}}'f_a \quad (i)$$

where f_a is the aromaticity and $(H/C)_{\text{ar}}'$ is the aromatic H/C ratio including phenolic hydrogen = $(1 - C_{\text{np,ar}})/C_{\text{ar}}$, $C_{\text{np,ar}}/C_{\text{ar}}$ being the fraction of non-protonated aromatic carbon corrected for phenols. For the bituminous coal samples, it has been assumed that the phenolic groups account for 60 % of the total oxygen consistent with much of the information in the literature (23).

Table 3 Carbon skeletal parameters derived from solid state ¹³C SPE NMR spectroscopy

SAMPLE	f_a (1)	$C_{\text{NP,AR}}/C$ (2)	$(H/C)_{\text{EL}}$ (3)	$(H/C)_{\text{AR}}^*$ (4)	$(H/C)_{\text{AL}}$ (5)
Snibston	0.77	0.46	0.76	0.40	1.8
Silkstone	0.79	0.52	0.74	0.34	2.0
Manton	0.81	0.53	0.74	0.35	2.1
Oakdale	0.87	0.53	0.61	0.40	2.1

Key

- (1): aromaticity, mole fraction of total sp² carbon.
- (2): mole fraction of non-protonated aromatic carbon over total carbon.
- (3): atomic H/C ratio derived from elemental analysis.
- (4): aromatic H/C ratio derived from (2), excluding phenolic OH.
- (5): aliphatic H/C derived by expression (i) in text.

The aliphatic H/C ratios derived using expression (i) are in the range, 1.8-2.1 (Table 3) which appears to be reasonably consistent with structural information derived from other techniques (23). The key finding is that, in the rank range from Snibston to Manton where %R_o increases from 0.47 to 0.79 (Table 1), there is a small increase in carbon aromaticity (0.79 to 0.81), but the fractions of non-protonated carbon (0.52-0.53, Table 3) and the atomic H/C ratios (Table 1) remain constant. It is difficult to derive unambiguously the fraction of bridgehead aromatic carbons from the total fraction of non-protonated aromatic carbons since the fractions of alkyl and heteroatom-attached carbons must be subtracted and this is beyond the scope of this investigation. However, the relatively small variations in O content (by difference, Table 1) of ca 2% and the similarity of the aromaticities and fractions of non-protonated carbon (Table 3) would suggest that the proportions of

bridgehead aromatic carbon vary by no more than 3-5 mole % carbon. However, this still might be significant given that there is a change of 9 mole % in going from naphthalene to phenanthrene. Thus, although the degree of condensation of the aromatic structure is not likely to change markedly or to an extent that can readily be detected by solid state ^{13}C NMR, it could well be that secondary factors, particularly the anisotropy of aromatic nuclei as reflected by the extent of non-covalent associative interactions are responsible for the variation in vitrinite reflectance.

ACKNOWLEDGEMENTS

The authors thank the the Science and Engineering Research Council (Grant no.GR/F/87264) and British Gas plc (CASE studentship for GDL) for financial support.

REFERENCES

1. Fu J., Sheng G., Xu J., Eglinton G., Gowar A.P., Jia R., Fan S. and Peng P. (1989). In *Advances in Organic Geochemistry 1989* (Edited by Durand B. and Behar F.), *Org. Geochem.* **16**, 93-104, Pergamon Press, Oxford.
2. Chaffee A.L., Hoover D.S., Johns R.B. and Schweighardt F.K. (1986) *In Biological Markers in the Sedimentary Record* (Edited by Johns R.B.), pp. 311-345. Elsevier, Amsterdam.
3. Mackenzie A.S. (1984) In *Advances in Petroleum Geochemistry* (Edited by Brooks J and Welte D.), Vol 1, pp. 115-214. Academic Press, London.
4. Radke M., Welte D.H. and Willsch H.(1982) *Geochim. Cosmochim. Acta* **46**, 1-10.
5. Radke M., Willsch H., Leythaeuser D and Teichmuller M. (1982) *Geochim. Cosmochim. Acta.* **46**, 1831-1848.
6. Radke M. and Welte D.H. (1983) *In Advances in Organic Geochemistry 1983* (eds. M. Bjoroy et al.), pp. 504-512. Wiley.
7. Michaelis W., Richnow H.H., Jenisch A., Schulze T. and Mycke B. (1989) *In Facets of Modern Biogeochemistry* (Eds Itterkkot V., Kempe S., Michaelis W. and Spitzzy), pp 389-402, Springer Verlag, Heidelberg.
8. Mycke B. and Michaelis W. (1986) *In Advances in Organic Geochemistry 1985* (eds. Leythaeuser D and Rullkottter J.), *Org. Geochem.* **10**, 847-858. Pergamon Press, Oxford.
9. Hayatsu R., Winans R.E., Scott R.G., Moore L.P. and Studier M.H. (1978) *Fuel* **57**, 541-548.
10. Youtcheff J.S., Given P.H., Baset Z. and Sundaram M.S. (1983) *Org. Geochem.* **5**, 157-164.
11. Monthieux M. and Landais P. (1987) *Fuel* **66**, 1703-1708.
12. Green T.K. and Larsen J.W. (1984) *Fuel* **63**, 1538-1547.
13. Nishioka M. (1992) *Fuel* **71**, 941-948
14. Kuehn D.W., Davies A., Snyder R.W., Starsinic M., Painter P.C., Havens J. and Koenig J.L. (1982) *Prepr. Am. Chem. Soc. Div. Fuel Chem.* **27**, 55-63.
15. Furimsky E. and Ripmeester J. (1983) *Fuel Process. Technol.* **7**, 191-202.
16. Russell N.J., Wilson M.A., Pugmire R.J. and Grant D.M. (1983) *Fuel* **62**, 601-605.
17. Carr A.D. and Williamson J.E. (1990) *In Advances in Organic Geochemistry 1989* (eds. Durand B. and Behar F.), *Org. Geochem.* **16**, 313-323. Pergamon Press, Oxford.
18. Franz J.A., Garcia R., Linchan J.C., Love G.D. and Snape C.E. (1992) *Energy & Fuels* **6**, 598-602.
19. Love G.D., Snape C.E. and Carr A.D. (1991) *Proc. Int. Conf. on Coal Sci.* (Newcastle), 64-67.
20. Snape C.E. and Love G.D. (1991) *Prep. Am. Chem. Soc. Div. Fuel Chem.* **36(3)**, 877-883.
21. Larsen J.W. and Mohammadi M. (1990) *Energy & Fuels* **4**, 107-110.
22. Lafferty C.J., Mitchell S.C., Garcia R. and Snape C.E. (1993) *Fuel* **72**, 367-372.
23. Love G.D., Law R.V. and Snape C.E. (1993) *Energy & Fuels*, in press.
24. Radke M., Willsch H. and Teichmuller M. (1990) *Org. Geochem.* **15**, 539-563
25. Jovancicevic B., Vitorovic D. and Wehner H. (1992) *Org. Geochem.* **18**, 511-519.
26. Love G.D. and Snape C. E., unpublished work.

Figure 1 : Yields of aliphatic (left) and aromatic (right) fractions produced from dichloromethane extraction -●- and from dichloromethane then pyridine extraction (cumulative) ○- for the vitrinite suite.

